Nonequilibrium Phase Transitions in Systems with Long-Range Interactions

Tarcísio N. Teles, Fernanda P. da C. Benetti, Renato Pakter, and Yan Levin

Instituto de Física, Universidade Federal do Rio Grande do Sul,
Caixa Postal 15051, CEP 91501-970, Porto Alegre, Rio Grande do Sul, Brazil
(Received 1 June 2012; published 4 December 2012)

We introduce a generalized Hamiltonian mean field model—an *XY* model with both linear and quadratic coupling between spins and explicit Hamiltonian dynamics. In addition to the usual paramagnetic and ferromagnetic phases, this model also possesses a nematic phase. The generalized Hamiltonian mean field model can be solved explicitly using Boltzmann-Gibbs statistical mechanics, in both canonical and microcanonical ensembles. However, when the resulting microcanonical phase diagram is compared with the one obtained using molecular dynamics simulations, it is found that the two are very different. We will present a dynamical theory which allows us to explicitly calculate the phase diagram obtained using molecular dynamics simulations without any adjustable parameters. The model illustrates the fundamental role played by dynamics as well the inadequacy of Boltzmann-Gibbs statistics for systems with long-range forces in the thermodynamic limit.

A fundamental concept in statistical mechanics, taught in a typical course, is the equivalence of ensembles [1]. One also learns that mean field theory becomes exact for systems with long-range (LR) interactions [2,3]. However, in order to have a well-defined thermodynamic limit, in this case, special care must be taken. The usual approach is to scale the strength of the two-body interaction potential with the number of particles in the system, N. This is the, so-called, Kac prescription—it makes the infinitely long-range two-body interaction infinitesimally weak [2]. The thermodynamic limit becomes well-defined, since both the kinetic and the potential contributions to the total energy now scale linearly with N, making the energy extensive. Over the last decade, however, it has become clear that both the ensemble equivalence and the exactness of mean field theory may fail for systems with LR interactions [4–6]. The phase-diagrams calculated using Boltzmann-Gibbs (BG) statistics in canonical and microcanonical ensembles do not always coincide [4]. Furthermore, molecular dynamics simulations, show that isolated LR interacting systems become trapped in quasistationary states (qSS), the lifetime of which diverges with the number of particles [7–15]. These qSS depend explicitly on the initial particle distribution.

The inapplicability of BG statistics to systems with LR forces in thermodynamic limit is a consequence of the ergodicity breaking. Scaling of two-body potentials with the number of particles—essential for the existence of a well-defined thermodynamic limit—destroys the correlations (collisions) between the particles [16] that drive normal short-range interacting systems towards the thermodynamic equilibrium. Relaxation to the stationary state of an LR system is, therefore, fundamentally different from the collisional (correlational) relaxation of normal gases and fluids. Collisionless relaxation relies on the collective

excitations and evaporative cooling driven by Landau damping [12,17]. The final stationary state reached by a collisionless system is intrinsically nonergodic [13,18]. It does not correspond to the maximum of the Boltzmann entropy. To exemplify this dichotomy, in this Letter, we introduce a new generalized Hamiltonian mean field model (GHMF)—a LR version of the model studied in Refs. [19,20]—which can be solved exactly using BG statistical mechanics. We will show that the equilibrium phase diagram predicted by the BG statistics in the microcanonical ensemble is very different from the one obtained using the molecular dynamics (MD) simulations. We will then construct a dynamical theory that correctly predicts the location and the order of the phase transitions observed in MD simulations.

The GHMF is described by the Hamiltonian

$$H(\theta_i, p_i) = \sum_{i=1}^{N} \frac{p_i^2}{2} + \frac{1}{2N} \sum_{i,j=1}^{N} [1 - \Delta \cos(\theta_i - \theta_j)$$
$$- (1 - \Delta) \cos(2\theta_i - 2\theta_j)], \quad (1)$$

where $\Delta \in [0, 1]$. The model can be thought of as either *XY* spins confined to a line, or as particles restricted to move on a circle. The latter interpretation is perhaps more convenient when discussing MD simulations with equations of motion given by: $\dot{\theta}_i = \partial H/\partial p_i$ and $\dot{p}_i = -\partial H/\partial \theta_i$.

We define the ferromagnetic and nematic order parameters as $m_1 = \frac{1}{N} \sum_{i=1}^{N} \cos\theta_i$ and $m_2 = \frac{1}{N} \sum_{i=1}^{N} \cos2\theta_i$, respectively. Using the usual statistical mechanics approach [5], we first calculate the microcanonical entropy for the GHMF.

Within BG statistical mechanics, all the thermodynamic information is encoded in the phase space volume accessible to the system with the total energy E

$$\Omega(E, N) = \int_{-\pi}^{\pi} \prod d\theta_i \int_{-\infty}^{\infty} \prod dp_i \delta(E - H(\theta_i, p_i)). \quad (2)$$

The integral in Eq. (2) can be divided into two parts—kinetic and configurational,

$$\Omega(E, N) = \int dK \Omega_{\text{kin}}(K) \Omega_{\text{conf}}(E - K), \quad (3)$$

where

$$\Omega_{\text{kin}}(K) = \int_{-\infty}^{\infty} \prod dp_i \delta\left(K - \frac{\sum p_i^2}{2}\right), \quad (4)$$

$$\Omega_{\text{conf}}(E - K) = \int_{-\pi}^{\pi} \prod d\theta_i \delta(E - K - U(\{\theta_i\})), \quad (5)$$

and U is the potential energy, second term in Eq. (1). Integrating over the momentum degrees of freedom, in the thermodynamic limit we obtain

$$\Omega_{\text{kin}}(K) = \exp\left[\frac{N}{2}\left(\ln\pi + \ln 2K - \ln\frac{N}{2} + 1\right)\right]. \quad (6)$$

The microcanonical entropy per particle is $s(\varepsilon) = \frac{1}{N} \ln\Omega(E, N)$,

$$s(\varepsilon) = \frac{1}{2} \ln 2\pi + \frac{1}{2} + \sup_\kappa\left[\frac{1}{2} \ln 2\kappa + \frac{1}{N} \ln\Omega_{\text{conf}}(N(\varepsilon - \kappa))\right], \quad (7)$$

where $\kappa \equiv K/N = (E - U)/N = \varepsilon - u$. Since the potential energy depends only on m_1 and m_2, we define

$$\Omega_m(m_1, m_2) = \int_{-\pi}^{\pi} \prod d\theta_i \delta\left(\sum \cos\theta_i - Nm_1\right)$$

$$\times \delta\left(\sum \cos 2\theta_i - Nm_2\right), \quad (8)$$

which using the Fourier representation of the delta function can be written as

$$\Omega_m(m_1, m_2) = \frac{1}{(2\pi)^2} \int_{-\infty}^{\infty} dx \int_{-\infty}^{\infty} dy \exp\Big\{N\Big[-ixm_1 - iym_2$$

$$+ \ln\Big(\Big(\int d\theta \exp(ix\cos\theta + iy\cos 2\theta)\Big)\Big)\Big]\Big\}. \quad (9)$$

The integral can be evaluated using the saddle-point method. The extremum corresponds to $(x^\star, y^\star)$, which must satisfy

$$m_1 = \frac{\int d\theta \cos\theta \exp[ix\cos\theta + iy\cos 2\theta]}{\int d\theta \exp[ix\cos\theta + iy\cos 2\theta]}, \quad (10)$$

$$m_2 = \frac{\int d\theta \cos 2\theta \exp[ix\cos\theta + iy\cos 2\theta]}{\int d\theta \exp[ix\cos\theta + iy\cos 2\theta]}. \quad (11)$$

Defining $a = ix^\star$ and $b = iy^\star$ and neglecting terms of order lower than N,

$$\frac{1}{N} \ln\Omega_m(m_1, m_2) = -m_1 a(m_1, m_2) - m_2 b(m_1, m_2)$$

$$+ \ln\left(\int d\theta \exp[a(m_1, m_2)\cos\theta + b(m_1, m_2)\cos 2\theta]\right). \quad (12)$$

In the thermodynamic limit, we may replace $\ln\Omega_{\text{conf}}(E - K)$ by $\ln\Omega_m(m_1, m_2)$ in Eq. (7). Furthermore, noting that $\kappa = \varepsilon - u$, where $u = (1 - \Delta m_1^2 - (1 - \Delta)m_2^2)/2$, the maximization can be taken with respect to m_1, m_2 instead of κ. The entropy per particle then becomes

$$s(\varepsilon) = \frac{1}{2} \ln 2\pi + \frac{1}{2} + \sup_{m_1, m_2}\Big\{\frac{1}{2} \ln[(2\varepsilon - 1 + \Delta m_1^2$$

$$+ (1 - \Delta)m_2^2)] - m_1 a(m_1, m_2) - m_2 b(m_1, m_2)$$

$$+ \ln\Big[\int d\theta \exp(a(m_1, m_2)\cos\theta + b(m_1, m_2)$$

$$\times \cos 2\theta)\Big]\Big\}. \quad (13)$$

with the equilibrium values of the order parameter $(m_1^\star, m_2^\star)$ given by

$$\frac{\Delta m_1^\star}{2\varepsilon - 1 + \Delta m_1^{\star 2} + (1 - \Delta)m_2^{\star 2}} = a(m_1^\star, m_2^\star), \quad (14)$$

$$\frac{(1 - \Delta)m_2^\star}{2\varepsilon - 1 + \Delta m_1^{\star 2} + (1 - \Delta)m_2^{\star 2}} = b(m_1^\star, m_2^\star). \quad (15)$$

Substituting these expressions into Eqs. (10) and (11), we find the equilibrium values of the order parameters

$$m_1 = \frac{\int_{-\pi}^{\pi} d\theta \cos\theta \exp\left[\frac{\Delta m_1 \cos\theta + (1-\Delta)m_2 \cos 2\theta}{2\varepsilon - 1 + \Delta m_1^2 + (1-\Delta)m_2^2}\right]}{\int_{-\pi}^{\pi} d\theta \exp\left[\frac{\Delta m_1 \cos\theta + (1-\Delta)m_2 \cos 2\theta}{2\varepsilon - 1 + \Delta m_1^2 + (1-\Delta)m_2^2}\right]}, \quad (16)$$

$$m_2 = \frac{\int_{-\pi}^{\pi} d\theta \cos 2\theta \exp\left[\frac{\Delta m_1 \cos\theta + (1-\Delta)m_2 \cos 2\theta}{2\varepsilon - 1 + \Delta m_1^2 + (1-\Delta)m_2^2}\right]}{\int_{-\pi}^{\pi} d\theta \exp\left[\frac{\Delta m_1 \cos\theta + (1-\Delta)m_2 \cos 2\theta}{2\varepsilon - 1 + \Delta m_1^2 + (1-\Delta)m_2^2}\right]}, \quad (17)$$

where for notational simplicity, we have dropped $\star$. In the case of a first order phase transition—more than one solution of Eqs. (16) and (17)—the equilibrium values of m_1 and m_2 will correspond to the ones that lead to the maximum entropy. The resulting microcanonical phase diagram is shown in Fig. 1.

Equation (2) requires that the system described by the Hamiltonian [Eq. (1)] is ergodic—has equal probability of visiting all possible microstates. To see if this is the case, we use MD simulations to study its dynamics. For the GHMF, we are interested to understand how an ordered (ferromagnetic or nematic) state can arise from an originally disordered homogeneous (paramagnetic) particle distribution $f_0(\theta, p) = \frac{1}{4\pi p_0} \Theta(\pi - |\theta|)\Theta(p_0 - |p|)$. The
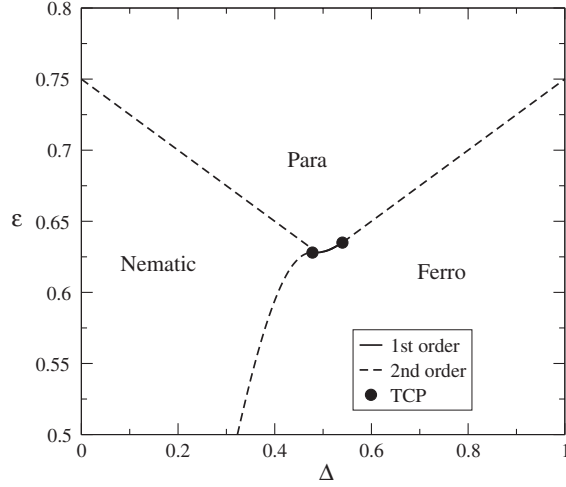
FIG. 1. Microcanonical phase diagram obtained using BG statistics. Solid circles are the two tricritical points.
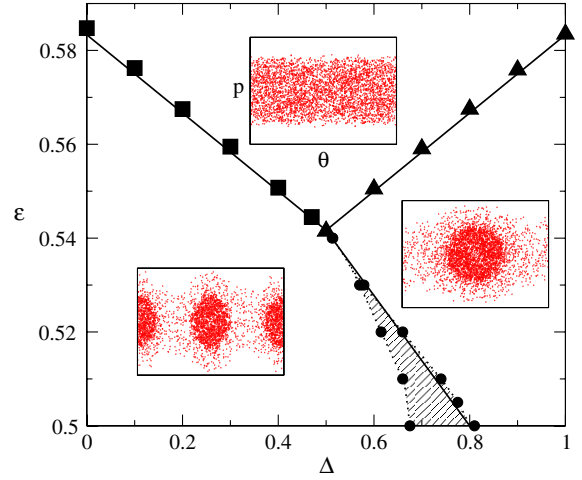

FIG. 2 (color online). The out-of-equilibrium phase diagram of the GHMF. The squares and triangles are simulation results for the qSS nematic-paramagnetic and para-ferromagnetic phase transitions, respectively. The shaded area represents the nematic-ferromagnetic transition region in which either phase occurs with equal probability. To the right of this region, the order is ferromagnetic, and to the left, nematic. Black solid lines are the theoretical predictions for the transitions. All transitions are first order. Insets show the phase space particle distribution in different phases. Notice the characteristic core-halo structure [15] inside both nematic and ferromagnetic phases. The simulations were performed with 2×10^6 particles for the paramagnetic-nematic and paramagnetic-ferromagnetic transition, and with 2×10^7 particles to locate the instability region between the nematic and ferromagnetic phases.

Hamilton's equations of motion reduce to a second order differential equation for θ_i,

$$\ddot{\theta}_i = F(\theta_i)$$
$$\equiv -\Delta m_1(t)\sin\theta_i(t) - 2(1-\Delta)m_2(t)\sin2\theta_i(t), \quad (18)$$

where $F(\theta)$ is the force acting on a particle located at θ, and where we have used the fact that $\langle\sin\theta(t)\rangle = \langle\sin2\theta(t)\rangle = 0$, throughout the dynamical evolution [15,21]. Comparing the phase diagram obtained using MD simulations, we see that it is very different from the prediction of the microcanonical BG statistical mechanics, see Fig. 2.

Besides occurring in different regions of the (ε, Δ) plane, the phase transitions predicted by the BG statistics are of the wrong order. While the transitions from paramagnetic to ferromagnetic or nematic phases are found to be second order, MD simulations show that these transitions are of first order. Furthermore, the second order phase transition line between the nematic and the ferromagnetic phase disappears completely and is replaced by a region of instability in which either phase can occur with equal probability.

To understand the results of MD simulations, one must forget equilibrium statistical mechanics and return to kinetic theory. In the thermodynamic limit, the dynamical evolution of the one-particle distribution function $f(\theta, p, t)$ of a system with long-range interactions is governed exactly by the Vlasov equation [22]. Vlasov dynamics is collisionless—the relaxation to equilibrium comes from Landau damping, a dynamical process in which individual particles gain energy from collective oscillations, while the oscillations are damped out. The one-particle energy of the GHMF is $\varepsilon = p^2/2 + 1 - \Delta m_1\cos(\theta) - (1-\Delta)m_2\cos(2\theta)$. Note that the initial particle distribution $f_0(\theta, p)$ has $m_1 = m_2 = 0$, so that it can be expressed as a function of ε. This means that $f_0(\theta, p)$ is a stationary

solution of the Vlasov equation. A phase transition in GHMF, therefore, can occur only after a dynamical instability. To explore the nonlinear stability of the GHMF, we consider a perturbation of the initial distribution, such that the maximum momentum $p_0 \to p_m(t) = p_0 + \sum_{n=0}^{\infty} A_n(t)\cos(n\theta)$. We define the generalized order parameters as

$$m_n(t) \equiv \langle\cos(n\theta)\rangle \equiv \int f(\theta, p, t)\cos(n\theta)dpd\theta, \quad (19)$$

where $f(\theta, p, t) = \frac{1}{4\pi p_0}\Theta(\pi - |\theta|)\Theta(p_m(t) - |p|)$. Note that this distribution preserves the phase space density, as is required by the Vlasov equation. Performing the integration in Eq. (19), we find that $m_n(t) = A_n(T)/2p_0$. Taking two temporal derivatives of $m_n(t)$, we obtain,

$$\ddot{m}_n = -n^2\langle p^2\cos(n\theta)\rangle - n\langle F(\theta)\sin(n\theta)\rangle, \quad (20)$$

where we have used the equation of motion, Eq. (18). Performing the averages using the distribution function $f(\theta, p, t)$, we obtain the equations of motion for the generalized order parameters,

$$\ddot{m}_1 + \left(\frac{12\varepsilon - 6 - \Delta}{2}\right)m_1 = f_1(m_1, m_2, m_3, m_4), \quad (21)$$

$$\ddot{m}_2 + 2(12\varepsilon + \Delta - 7)m_2 = f_2(m_1, m_2, m_3, m_4), \quad (22)$$

$$\ddot{m}_3 + 27(2\varepsilon - 1)m_3 = f_3(m_1, m_2, m_3, m_4), \quad (23)$$

$$\ddot{m}_4 + 48(2\varepsilon - 1)m_4 = f_4(m_1, m_2, m_3, m_4), \quad (24)$$

where

$$f_1 = m_1 m_2 \left(1 - \frac{3\Delta}{2}\right) + (\Delta - 1)m_2 m_3 - 3(2\varepsilon - 1)$$
$$\times \{m_1^3 + m_1^2 m_3 + m_3[m_2(2 + m_2) + 2(1 + m_2)m_4]$$
$$+ 2m_1[m_2 + m_2^2 + m_3^2 + m_2 m_4 + m_4^2]\}, \quad (25)$$

$$f_2 = \Delta(m_1^2 - m_1 m_3 + 2m_2 m_4) - 2m_2 m_4$$
$$- 12(2\varepsilon - 1)[m_2^3 + m_3^2 m_4 + 2m_1 m_3(1 + m_2 + m_4)$$
$$+ m_1^2(1 + 2m_2 + m_4) + 2m_2(m_3^2 + m_4 + m_4^2)], \quad (26)$$

$$f_3 = \frac{3m_1}{2}[(2 - \Delta)m_2 - \Delta m_4] - 9(2\varepsilon - 1)\{m_1^3 + 6m_1^2 m_3$$
$$+ 3m_1[m_2(2 + m_2) + 2(1 + m_2)m_4]$$
$$+ 3m_3[m_3^2 + 2(m_2^2 + m_2 m_4 + m_4^2)]\}, \quad (27)$$

$$f_4 = 2\Delta m_1 m_3 - 4(\Delta - 1)m_2^2 - 48(2\varepsilon - 1)[2m_1(1 + m_2)m_3$$
$$+ m_2(m_2 + m_3^2) + 2(m_2^2 + m_3^2)m_4 + m_4^3$$
$$+ m_1^2(m_2 + 2m_4)]. \quad (28)$$

We have restricted ourselves to the first four generalized order parameters, since these are already sufficient to understand the phase diagram obtained using MD simulations. Note that the right hand sides of Eqs. (21)–(24) are nonlinear functions, so that the transition from paramagnetic-to-ferromagnetic or paramagnetic-to-nematic phases is determined by the linear stability of these equations. Furthermore, all the order parameters with $n > 2$ are linearly stable. Equations (21) and (22) show that the paramagnetic phase becomes unstable to ferromagnetic ordering when $12\varepsilon - 6 - \Delta < 0$ and to nematic ordering when $12\varepsilon + \Delta - 7 < 0$. The two stability lines agree perfectly with the results of MD simulations, see Fig. 2. It is important to note that m_3 and m_4 always remain linearly stable (recall that $\varepsilon > 0.5$ for the initial distribution).

Linear stability analysis, however, is not sufficient to determine the order of the phase transitions for which the full nonlinear equations must be considered. We first note that Eqs. (21)–(24) are conservative, they do not account for the Landau damping that is responsible for the relaxation to equilibrium and formation of the core-halo structures [15], like the ones shown in the insets of Fig. 2. Phenomenologically, Landau damping can be included in

Eqs. (21)–(24) by introducing terms linear in $\dot{m}_n$. The relaxation will then proceed towards the fixed points of Eqs. (21)–(24) which can be calculated explicitly. We find that when either transition line is crossed, the system evolves either to nematic ($m_1 = 0$, $m_2 \neq 0$) or ferromagnetic ($m_1 \neq 0$, $m_2 \neq 0$) fixed points. When crossing the paramagnetic-nematic phase transition line, ($\Delta < 0.5$), the order parameter m_1 remains zero, while m_2 jumps by $\sqrt{\frac{5\sqrt{43}}{18} - \frac{29}{18}} \approx 0.459$, independent of Δ. This theoretical prediction is in excellent agreement with the results of MD simulation which see a jump in the nematic order parameter of 0.45, characterizing a strong first-order phase transition, see Fig. 3. When the paramagnetic-ferromagnetic line is crossed ($\Delta > 0.5$), both m_1 and m_2 experience a jump. For $\Delta = 0.6$, the theory predicts the jumps to be 0.5102 and -0.1861, for the ferromagnetic and nematic parameters, respectively, while the simulations find 0.41 and -0.10. For $\Delta = 1$, the theory predicts the respective jumps to be 0.555391 and -0.1129, while the simulations find 0.45 and -0.07. It is interesting to note that while for the nematic transition the jump in m_2 is universal—independent of Δ—for the ferromagnetic transition, this is not the case.

What will determine the transition between nematic and ferromagnetic phases? Deep inside the nematic and ferromagnetic phases, Eqs. (21)–(24) possess both stable nematic ($m_1 = 0$, $m_2 \neq 0$) and ferromagnetic fixed points ($m_1 \neq 0$, $m_2 \neq 0$). Which of these fixed points is reached first will depend on the initial condition. Starting from a paramagnetic distribution f_0, in the unstable region of the phase diagram, both m_1 and m_2 will grow with time. Equations (21) and (22) show that the rate of growth of the two order parameters are, in general, very different, while $m_1 \sim e^{\lambda_1 t}$, where $\lambda_1 = \sqrt{(6 + \Delta - 12\varepsilon)/2}$, the nematic order parameter grows as $m_2 \sim e^{\lambda_2 t}$, with $\lambda_2 = \sqrt{14 - 24\varepsilon - 2\Delta}$. If the nematic order parameter first
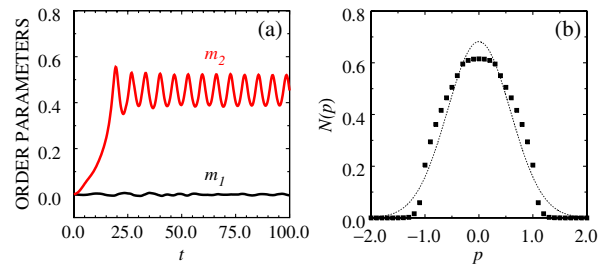

FIG. 3 (color online). Panel (a) shows the growth and saturation of the order parameter m_2 across the paramagnetic-nematic transition obtained using MD simulations. The predicted theoretical value is $m_2 = 0.459$, which is in excellent agreement with the simulations. In panel (b), the symbols are the momentum distribution in the qSS obtained using MD, while the solid line depicts the corresponding Maxwell—Boltzmann distribution to which the systems should relax in the infinite time limit. The parameters are $\Delta = 0.2$ and $u = 0.567$.

reaches the value characteristic of the nematic fixed point, then nematic order will be established, otherwise the phase will be ferromagnetic. Therefore, we expect that the nematic-ferromagnetic transition line should be given by $\lambda_1 = \lambda_2$ (solid line between nematic and ferromagnetic phases in Fig. 2). This is indeed where the instability characterizing nematic-to-ferromagnetic region is found to be, see Fig. 2.

We have introduced a generalized Hamiltonian mean field model. In addition to the usual paramagnetic and ferromagnetic phases, this model also possesses a nematic phase. We have obtained the phase diagram of the GHMF using three different methods: BG statistical mechanics, MD simulations, and a new dynamical theory introduced in this Letter. The model exemplifies the failure of BG statistics to describe isolated systems with LR interactions, in the thermodynamic limit. This is the first time that a complex (multiphase) out-of-equilibrium phase diagram for quasistationary states has been calculated analytically for a system with LR interactions.

[1] K. Huang, *Statistical Mechanics* (John Wiley & Sons, New York, 1987), 2nd ed.; L. E. Reichl, *A Modern Course In Statistical Physics* (Wiley-Interscience, New York, 1998), 2nd ed.

[2] M. Kac, Phys. Fluids **2**, 8 (1959); M. Kac, G. E. Uhlenbeck, and P. C. Hemmer, J. Math. Phys. (N.Y.) **4**, 216 (1963); G. A. Baker, Phys. Rev. **130**, 1406 (1963).

[3] H. E. Stanley, *Introduction to Phase Transitions and Critical Phenomena* (Oxford University Press, New York, 1971).

[4] J. Barré, D. Mukamel, and S. Ruffo, Phys. Rev. Lett. **87**, 030601 (2001).

[5] A. Campa, T. Dauxois, and S. Ruffo, Phys. Rep. **480**, 57 (2009).

[6] T. M. R. Filho, M. A. Amato, and A. Figueiredo, J. Phys. A **42**, 165 001 (2009).

[7] V. Latora, A. Rapisarda, and S. Ruffo, Phys. Rev. Lett. **83**, 2104 (1999).

[8] Y. Y. Yamaguchi, J. Barré, F. Bouchet, T. Dauxois, and S. Ruffo, Physica (Amsterdam) **337**, 36 (2004).

[9] A. Antoniazzi, D. Fanelli, S. Ruffo, and Y. Y. Yamaguchi, Phys. Rev. Lett. **99**, 040601 (2007).

[10] M. Joyce and T. Worrakitpoonpon, Phys. Rev. E **84**, 011139 (2011).

[11] K. Jain, F. Bouchet, and D. Mukamel, J. Stat. Mech. (2007) P11008.

[12] Y. Levin, R. Pakter, and T. N. Teles, Phys. Rev. Lett. **100**, 040604 (2008).

[13] T. N. Teles, Y. Levin, R. Pakter, and F. B. Rizzato, J. Stat. Mech. (2010) P05007.

[14] T. N. Teles, Y. Levin, and R. Pakter, Mon. Not. R. Astron. Soc. **417**, L21 (2011).

[15] R. Pakter and Y. Levin, Phys. Rev. Lett. **106**, 200603 (2011).

[16] Y. Levin, Rep. Prog. Phys. **65**, 1577 (2002).

[17] L. Landau, J. Phys. (Moscow) **10**, 25 (1946).

[18] F. P. da C. Benetti , T. N. Teles, R. Pakter, and Y. Levin, Phys. Rev. Lett. **108**, 140601 (2012).

[19] F. C. Poderoso, J. J. Arenzon, and Y. Levin, Phys. Rev. Lett. **106**, 067202 (2011).

[20] D. H. Lee and G. Grinstein, Phys. Rev. Lett. **55**, 541 (1985).

[21] T. M. R. Filho, M. A. Amato, and A. Figueiredo, Phys. Rev. E **85**, 062103 (2012).

[22] W. Braun and K. Hepp, Commun. Math. Phys. **56**, 101 (1977).